Quantifying Isolated Pore Space in Geological Barrier Materials

Qinhong Hu[1], Qiming Wang[1], Prince Oware[1], Tristan Tom[1], Yukio Tachi[2], Fukatsu Yuta[2], Jan Ilavsky[3], Jonathan Almer[3], and Jun-Sang Park[3]

[1]University of Texas at Arlington
[2]Japan Atomic Energy Agency
[3]Argonne National Laboratory

November 21, 2022

Abstract

Pore connectivity, a topological characteristic of pore structure, is oftentimes more important than the geometrical aspects in controlling fluid flow and mass transport in porous natural rocks as well as their associated utilities in energy and environmental stewardship. A different extent of pore connectivity can be reflected in the proportion of isolated pore space not connected to the surface of natural rocks. This work presents the multi-approach and multi-scale laboratory studies to investigating the proportion of isolated pore space of, and its resultant anomalous fluid flow and radionuclide movement in, generic geological barrier materials (clay sediment, crystalline rock, salt rock, shale, tuff). The samples include clay sediments of Wakkanai formation at Horonobe underground research center in Hokkaido of Japan, Opalinus clay of Mt. Terri Underground Research Laboratory as well as granodiorite from the Grimsel Test Site in Switzerland, salt rock from Waste Isolation Pilot Plant in New Mexico, various shales (Barnett, Eagle Ford and Wolfcamp from Texas), and welded tuff in Yucca Mountain in Nevada. Working with sample sizes from <75 µm to several centimeters, the experimental approaches include the independent quantification of both (1) surface-accessible pore space with various probing fluids (e.g., helium in expansion, water in vacuum saturation and nuclear magnetic resonance, mercury in intrusion porosimetry, nitrogen in gas physisorption, and Wood's metal in high-pressure impregnation and micron-scale tracer mapping using laser ablation-ICP-MS); and (2) total (both connected and isolated) porosity by small angle X-ray scattering. In summary, our evolving complementary approaches provide a rich toolbox for tackling the pore structure characteristics in geological barrier materials, and associated fluid flow & radionuclide transport, implicated in their long-term performance in natural and engineered systems of a nuclear waste repository.

Quantifying isolated pore space in geological barrier materials

(Max) Qinhong Hu, Qiming Wang, Prince Oware, Tristan Tom, Yukio Tachi, Yuta Fukatsu, Jan Ilavsky, Jonathan Almer, Jun-Sang Park

University of Texas at Arlington; Japan Atomic Energy Agency; Argonne National Laboratory

PRESENTED AT:

AGU FALL MEETING
Online Everywhere | 1–17 December 2020

RATIONAL AND EARLY WORK

Historical Evolution of Major Research Thrusts in the Environment, Energy, and Resources Studies

- Air and surface water contamination (1950s–1980s)
- Environmentalism movement (since 1960s)

involves clay materials & fractured media

- Soil contamination (1960s–present)
- Geothermal energy exploitation (1974–present)
- Tight sands and coalbed methane (1976–present)
- Geological repository of high-level nuclear waste (1978–present)
- Groundwater remediation and Superfund (1980–present)
- Carbon sequestration (1997–present)
- Petroleum production in shale gas and oil reservoirs (1981; 2008–present)
- Gas (methane) hydrate (2005–present)

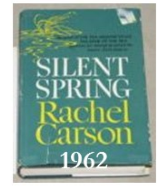

1970

1977

UNIVERSITY OF TEXAS–ARLINGTON

Nuclear Power Plants Worldwide

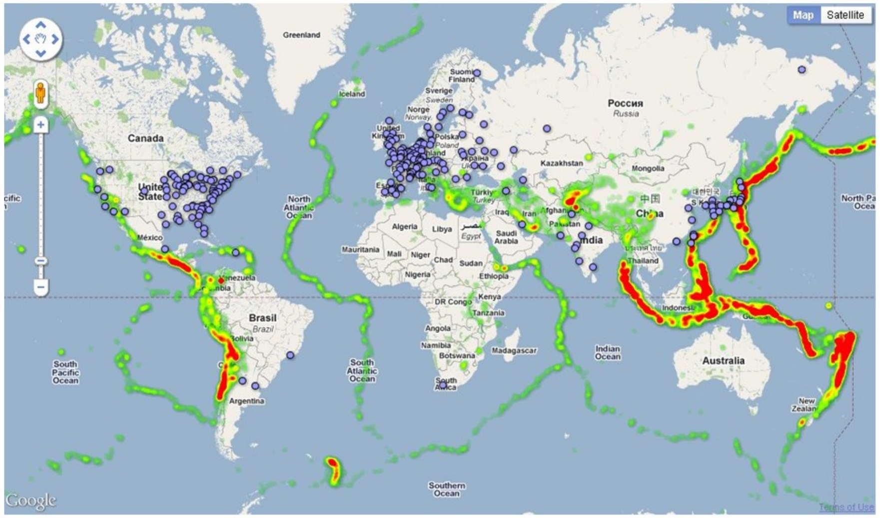

http://www.targetmap.com/viewer.aspx?reportId=4850

- **~35** countries
- **449** nuclear power reactors in operation
- 53 reactors under construction
- **5%** of world energy and **15%** of the world's electricity

http://www.iaea.org/pris/Home.aspx

UNIVERSITY OF TEXAS-ARLINGTON

Annual production of spent nuclear fuel: 10,000 MT

Nuclear Power and Geological Repository in Major Countries

Country	Operating plants in 2010 (2019)	Nuclear electricity generation in 2006 (2019) (billions kWh)	Nuclear electricity reliance (%)	Nuclear electricity of world total (%)	Projected repository operation
Belgium	7 (7)	44.3 (41.3)	54 (47.6)	1.7 (1.6)	between 2035–2080
Canada	18 (19)	92.4 (95.5)	18 (14.9)	3.5 (3.8)	after 2034
China	11 (48)	51.8 (348)	2.1 (4.9)	1.9 (13.8)	at earliest 2040
Czech Republic	6 (6)	24.5 (28.6)	32 (35.2)	0.9 (1.1)	after 2030
Finland	4 (4)	22 (22.9)	30 (34.7)	0.8 (0.9)	Olkiluoto in 2020; construc. in 2004; license in 2015; emplacement in 2023
France	59 (56)	429 (380)	76 (70.6)	16 (15.0)	by 2025
Germany	17 (6)	159 (0)	28 (0)	6.0 (0)	no projected date
India	18 (22)	15.6 (40.7)	2.0 (3.2)	0.6 (1.6)	TBD
Japan	53 (33)	292 (65.6)	25 (7.5)	11 (2.6)	at earliest 2035
Korea (South)	20 (24)	141 (137)	36 (26.2)	5.3 (5.5)	TBD
Russia	31 (38)	144 (209)	17 (19.7)	5.4 (8.3)	after 2025
Slovakia	4 (4)	16.6 (15.4)	56 (53.9)	0.6 (0.61)	TBD
Spain	8 (7)	57.4 (55.9)	18 (21.4)	2.2 (2.2)	TBD
Sweden	10 (7)	65.1 (55.9)	42 (21.4)	2.4 (2.2)	Forsmark, license applied in 2011
Switzerland	5 (4)	26.4 (16.6)	39 (23.9)	1.0 (0.66)	after 2050
Ukraine	15 (15)	84.8 (83.0)	47 (53.9)	3.2 (3.3)	after 2020
United Kingdom	19 (15)	69.2 (51.0)	13 (15.6)	2.6 (2.0)	TBD
United States	104 (95)	787 (809)	20 (19.7)	30 (32.0)	Indefinite after 2008

UNIVERSITY OF TEXAS-ARLINGTON

Geological Repository: Barrier (Host Rocks and Buffer) Materials

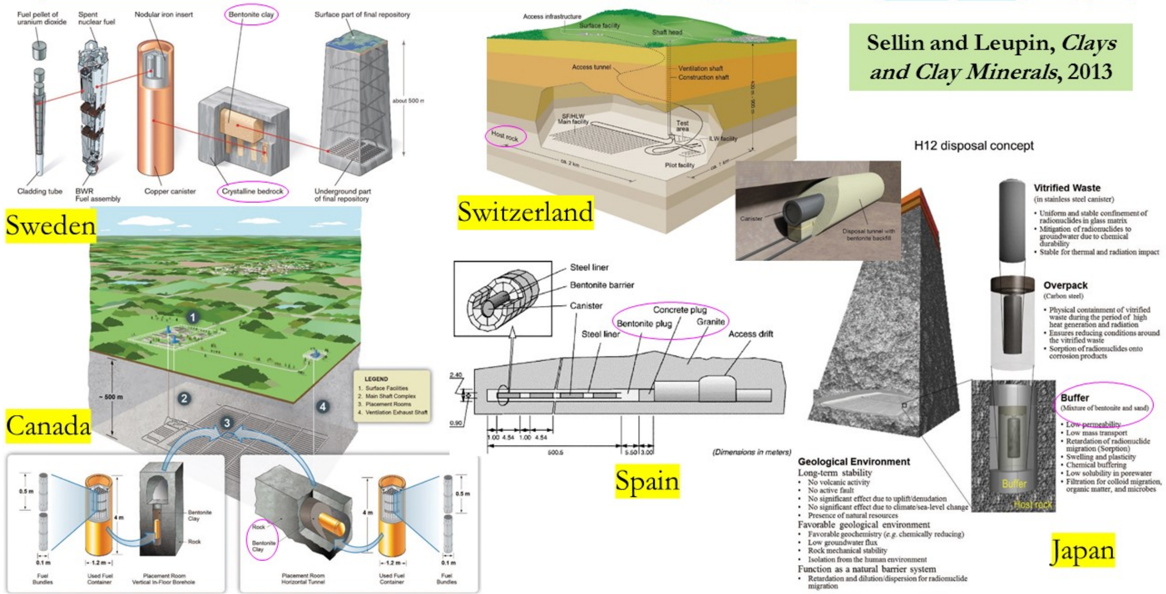

Sellin and Leupin, *Clays and Clay Minerals*, 2013

Las Vegas, Nevada Test Site and Yucca Mountain

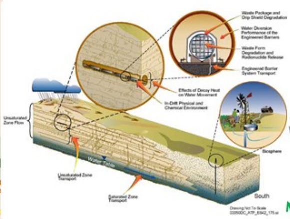

Yucca Mountain Project (1970 – 2008)

828 underground tests conducted between 1951 and 1992

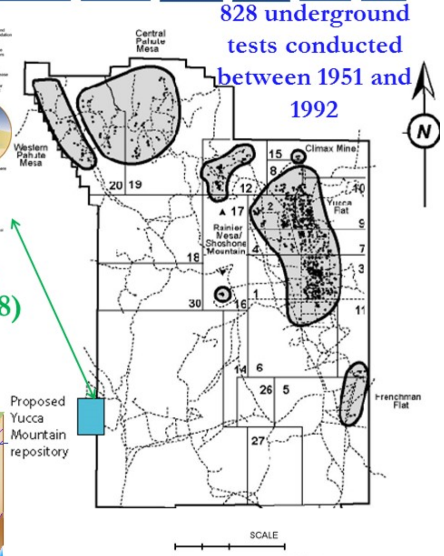

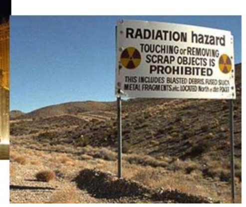

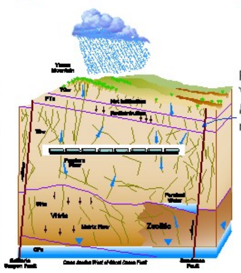

UNIVERSITY OF TEXAS–ARLINGTON

Earlier Fracture-Matrix Interaction Studies

Field observation (preferential flow in a fracture network) of dye distribution in unsaturated fractured tuff at Yucca Mt.

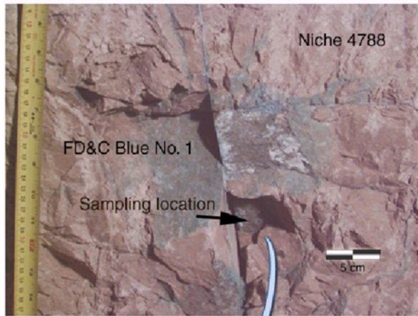

Exploratory Studies Facility (ESF); 1997

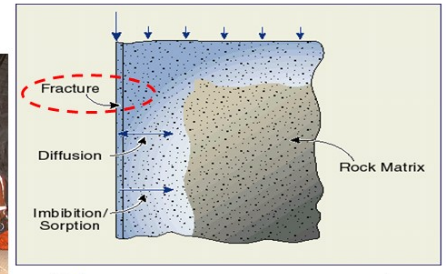

Rock milling in 1998

My work on fracture-matrix interaction starts with this rock

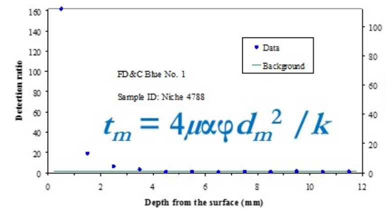

UNIVERSITY OF TEXAS-ARLINGTON

Hu et al., JCH, 2001; VZJ, 2002

Imbibition in Fractured Rock: Sorptivity and Permeability

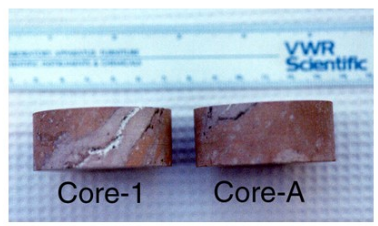

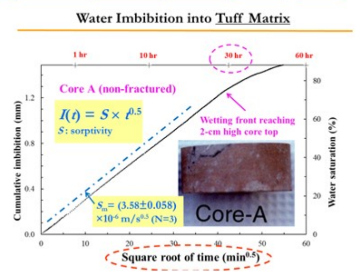

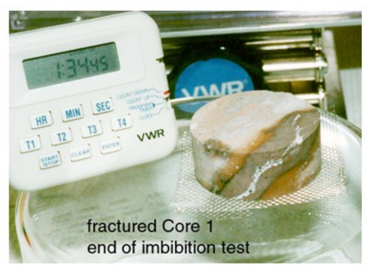

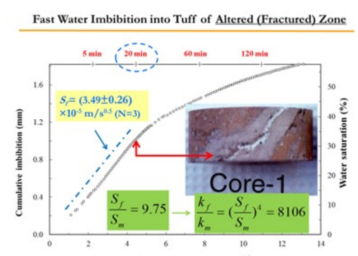

UNIVERSITY OF TEXAS-ARLINGTON

Hu et al., JH, 2001; VZJ, 2004

Laboratory Tracer Tests and Penetration Delineation

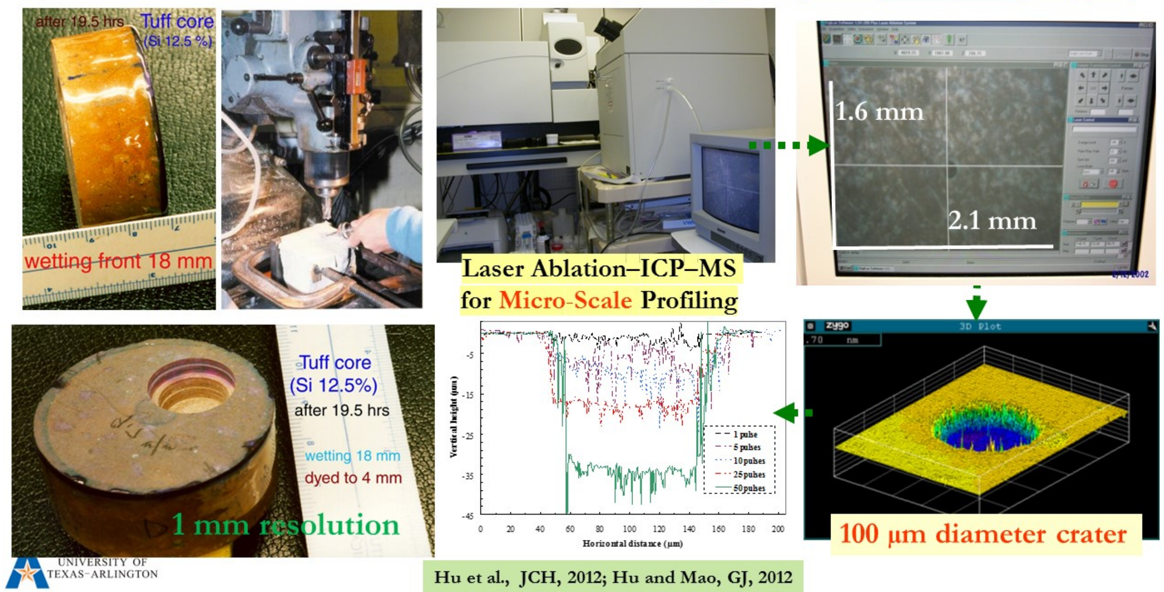

SAMPLES AND METHODOLOGIES

A Variety of Generic Geological Media: Host Rocks and Barrier Materials

Sample	Topopah Spring Welded Tuff	Marcellus Shale	Mancos Shale	Wolfcamp Shale	Salt Rock	Cement / Concrete
Source	Yucca Mtn., NV	Centre County, PA	San Juan Co., NM	Midland County, TX	Carlsbad, NM	LLNL; EPA

Sample	Gray Chalk	Wakkanai Mudstone	Boom Clay	Grimsel Granodiorite	Granite	Opalinus Clay
Source	Negev Desert, Israel	Horonobe Underground Res. Center, Hokkaido, Japan	The HADES Underground Res. Lab., Belgium	Grimsel, Switzerland	Stripa mine, Sweden	Mt. Terri Underground Research Laboratory, Switzerland

Sample	Silica Sand	Berea Sandstone	Na-rich Montmorillonite	Illite	Kaolin	Chlorite
Source	Ottawa, IL	Berea Quarry, OH	Crook County, WY	Silver Hill, MT	Twiggs County, GA	El Dorado County, CA

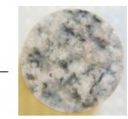

UNIVERSITY OF TEXAS–ARLINGTON

DOE-Nuclear Energy University Program: "Reduced diffusion and enhanced retention of multiple radionuclides from pore structure characterization of barrier materials for enhanced repository performance"

Pore Structure: Geometry and Topology

Percolation theory: the mathematics of how macroscopic properties emerge from local (microscopic) connections

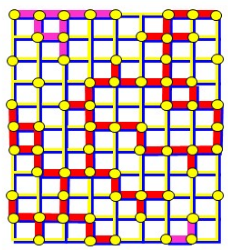

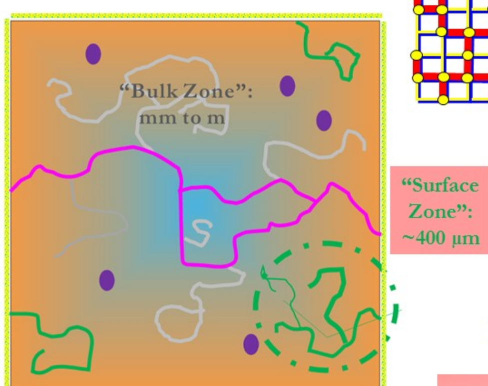

UNIVERSITY OF TEXAS–ARLINGTON

Sample surface

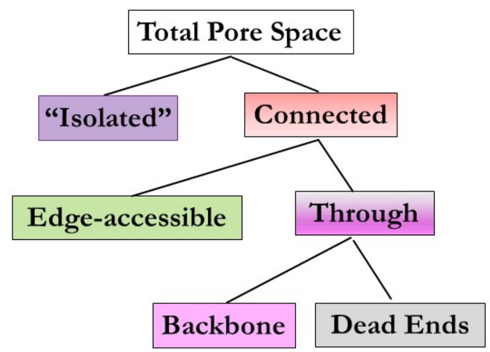

for mudrock

Hu et al., JGR, 2015

Effective porosity/Total porosity (ϕ_e / ϕ)

"Surface Zone": ~70% "Bulk Zone": ~0.1%

Multiple Approaches to Studying Pore Structure (Geometry and Topology)

- Vacuum saturation, liquid displacement, pycnometry, and enveloping methods of gas or hydrophilic / hydrophobic fluids (DIW; API brine; n-decane; toluene; isopropyl alcohol IPA; tetrahydrofuran THF; dimethylformamide DMF; crude oil) for fluid-accessible effective porosity of a range of sample sizes (μm – 10 cm)
- Fluid (DIW; API brine; n-decane; IPA) and tracer imbibition (bedding direction; initial fluid saturation; HPHT)
- Edge-accessible porosity after tracer vacuum-saturation and high-pressure intrusion
- Liquid and gas diffusion, under ambient and high-pressure / high-temperature conditions
- Mercury Intrusion Porosimetry
- Low-pressure gas adsorption isotherm and hysteresis
- Water vapor adsorption isotherm and hysteresis
- Nuclear Magnetic Resonance Cryoporometry
- Ar ion milling Field Emission-SEM (FE-SEM) and QEMSCAN (Quantitative Evaluation of Materials by Scanning) mapping, correlated with tracer mapping to study Dalmatian wettability and connectivity of shale pore systems
- 2-D imaging/mapping after Wood's metal impregnation
- Microtomography (high-resolution, synchrotron, nano-CT)
- Focused Ion Beam/SEM (FIB-SEM) imaging
- Small-Angle Neutron Scattering (U)SANS
- Small-Angle X-Ray Scattering (U)SAXS
- Pore-scale network modeling
- Physics-based production decline analyses

UNIVERSITY OF TEXAS–ARLINGTON

Hu et al., Hedberg Conference, 2010

A Range of Sample Sizes for Different Tests

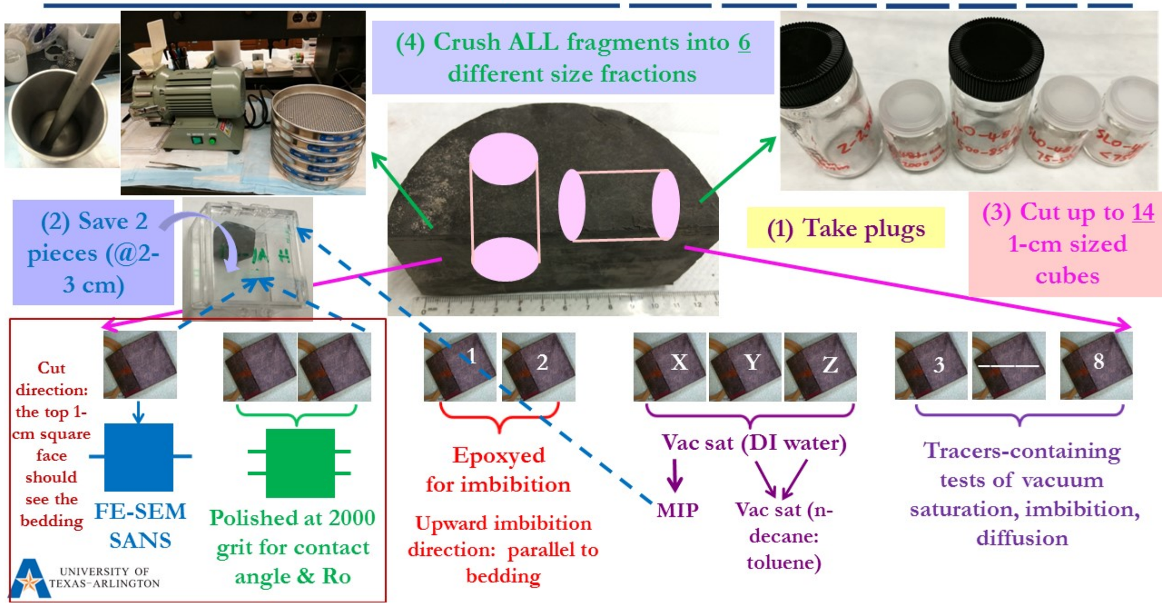

A Range of Sample Sizes for Pore Structure Characterization

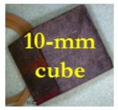

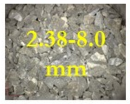

Size designation	Sieve mesh	Size fraction (diameter)	Equivalent spherical dia. (µm)	Equivalent spherical dia. (mm)
Cylinder / Plug		2.54 cm dia.; any height (e.g., 3 cm)	*(24394)*	*(24.39)*
Cube		1.0 cm	9086	9.086
Size X	8 mm to #8	2.38 - 8.0 mm	5180	5.180
GRI+	#8 to #12	1.70 - 2.38 mm	2030	2.030
Size A	#12 to #20	841 - 1700 µm	1271	1.271
GRI	#20 to #35	500 - 841 µm	671	0.671
Size B	#35 to #80	177 - 500 µm	339	0.339
Size C	#80 to #200	75 - 177 µm	126	0.126
Powder	<#200	< 75 µm	< 75	< 0.075
Size D	#200 to #625	20 - 75 µm	47.5	0.0475
Size E	<#635	<20 µm	<20	<0.02

GRI: Gas Research Institute

UNIVERSITY OF TEXAS–ARLINGTON

RESULTS: PYCNOMETRY, POROSIMETRY, AND TRACER MAPPING

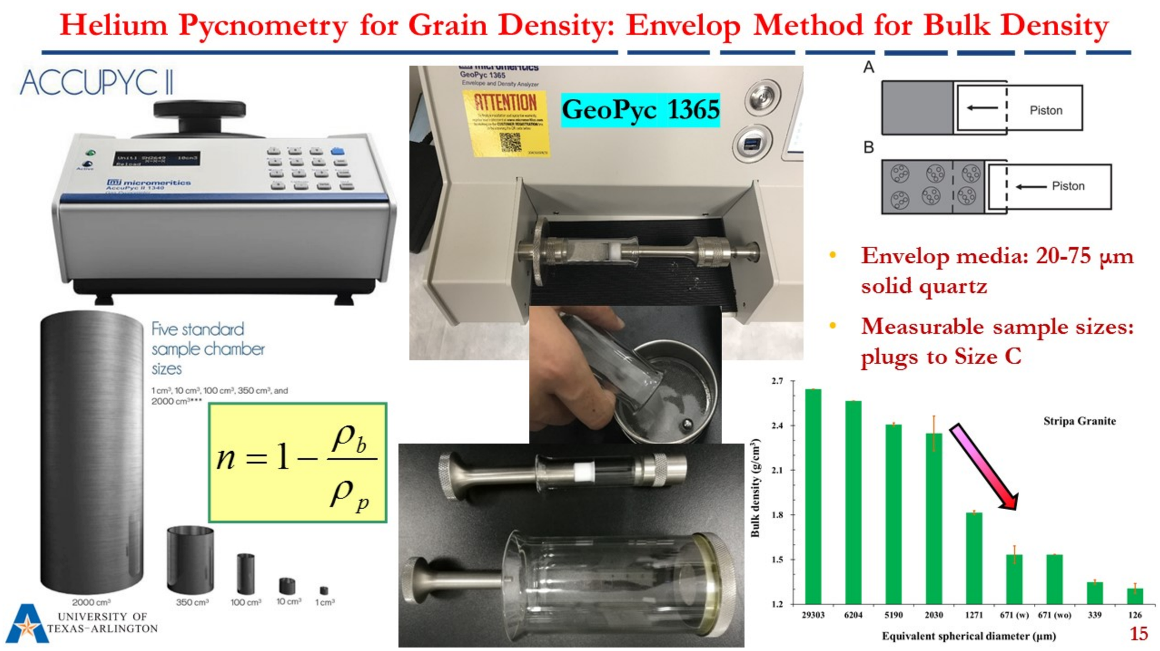

Multiple nm-µm Pore Systems of Mudrock

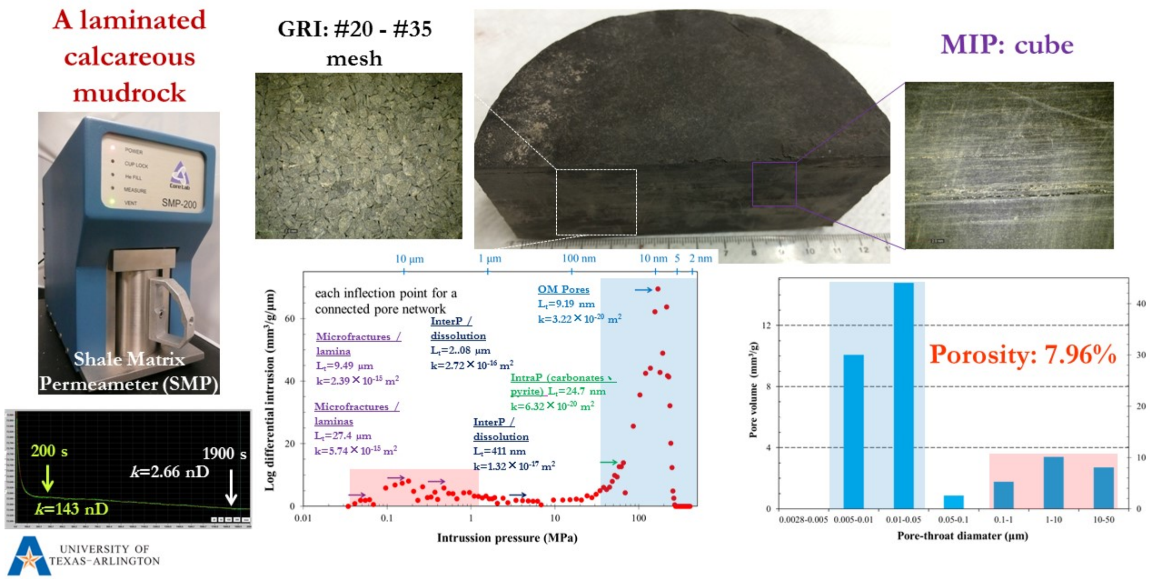

Pore-Throat Size Distribution and Pore Connectivity

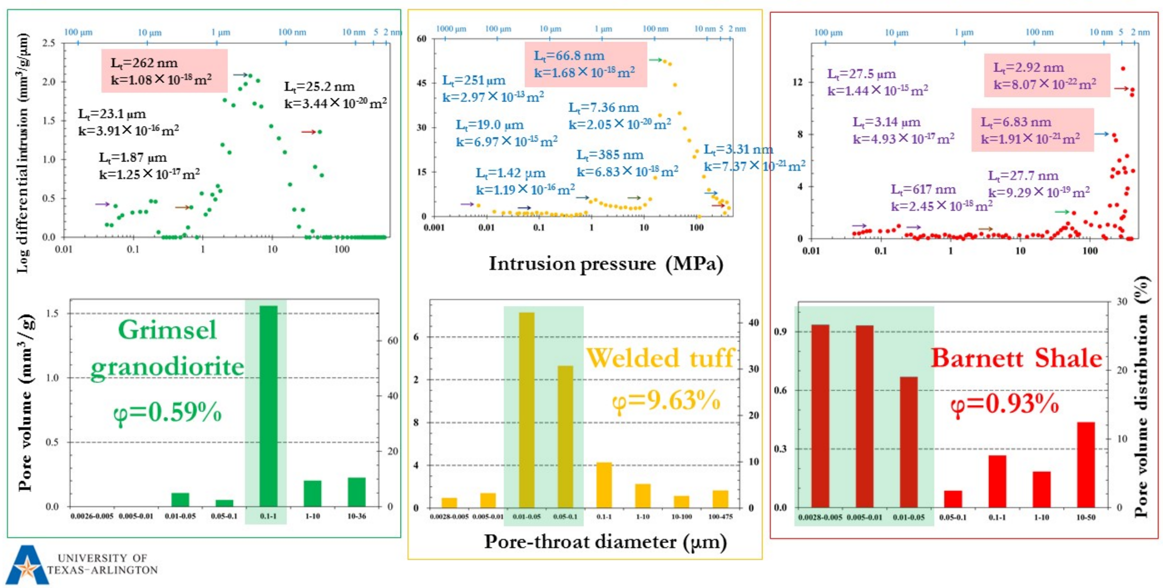

MIP Analyses of Pore Structure and Network: Barnett Shale

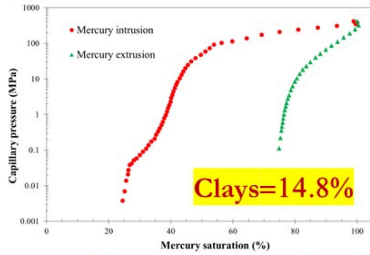

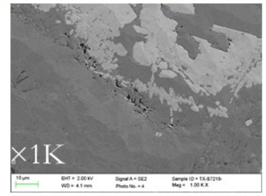

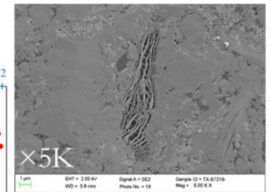

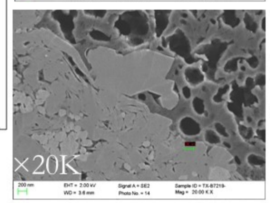

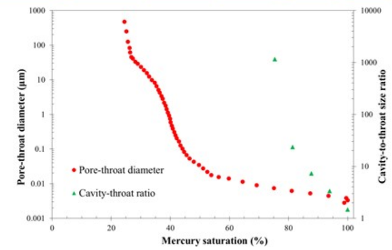

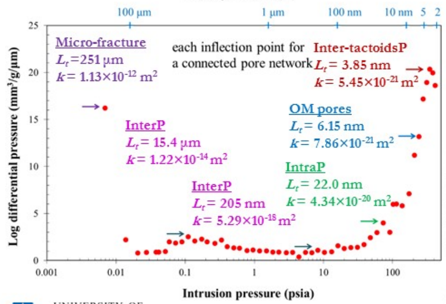

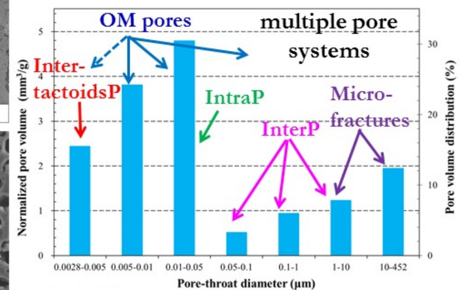

ϕ=5.09%

UNIVERSITY OF TEXAS–ARLINGTON

Clay Structure and Pore Space at Different Scales

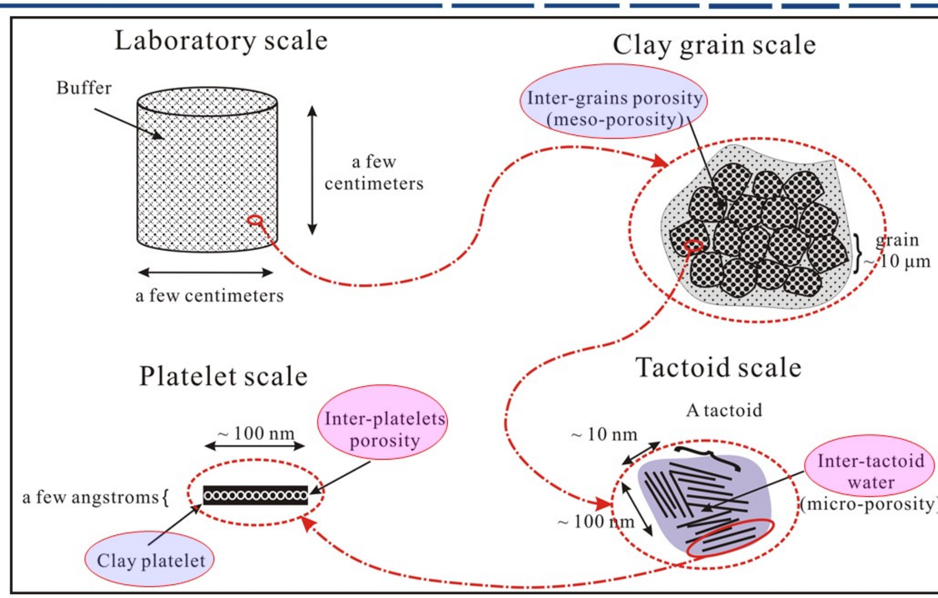

UNIVERSITY OF TEXAS–ARLINGTON

Wettability-based Fluids and Tracers

- Groundwater simulate [5 mM $Ca(NO_3)_2$; water-wet]
  - ✓ I^-, Br^- (0.181 nm)
  - ✓ ReO_4^- (0.553 nm), MoO_4^{2-} (RuO_4^-, SeO_4^{2-}, CrO_4^{2-})
  - ✓ 0.313 nm Cs^+, 0.211 nm Co^{2+}, 0.245 nm Sm^{3+} (Eu^{3+})

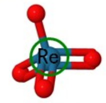

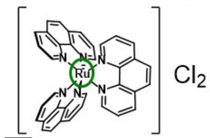

$C_{36}H_{24}N_6Ru_1Cl_2$

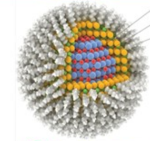

CdS (5–10 nm)

- API brine (8 wt% NaCl+2 wt% $CaCl_2$) [water-wet]
  - ✓ ReO_4^- (0.553 nm)
  - ✓ Anionic Sb-complex (0.89 nm)
  - ✓ Cationic Ru-complex (1.0 nm)
  - ✓ CdS nanoparticles (5–10 nm)

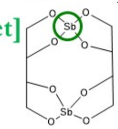

0.23 nm | 1.393 nm × 0.287 nm × 0.178 nm

$CH_3(CH_2)_8CH_2I$

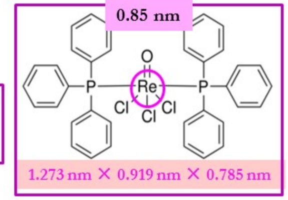

- n-decane: toluene [oil-wet]
  - ✓ Organic-I (1-iododecane)
  - ✓ Organic-Re [trichlorooxobis(triphenylphosphine)rhenium(V)]
  - ✓ CeF_3 nanoparticles (10–12 nm)
- IPA [zewittering]
  - ✓ Ru-complex (2.42 nm)

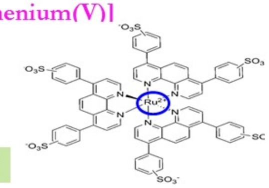

UNIVERSITY OF TEXAS–ARLINGTON

Hu et al., J. Nano. Nanotech., 2017

Different Tracer Tests for Process-Level Understanding

Imbibition

Diffusion

Laser Ablation-Inductively Coupled Plasma-Mass Spectrometry (LA-ICP-MS)

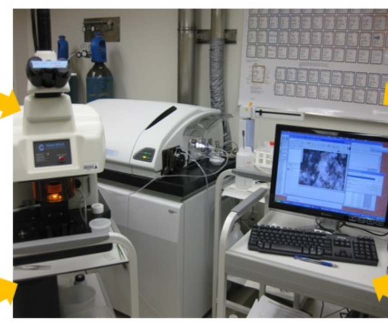

Hu et al., *VZJ*, 2004; *GJ*, 2012

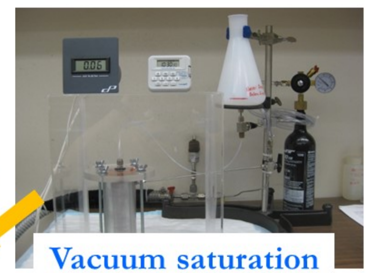

Vacuum saturation

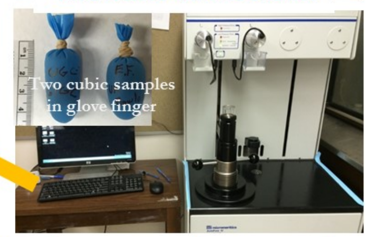

High-pressure impregnation

UNIVERSITY OF TEXAS–ARLINGTON

Unique Dual-Connectivity Zones of Mudrock: Multiple Evidence

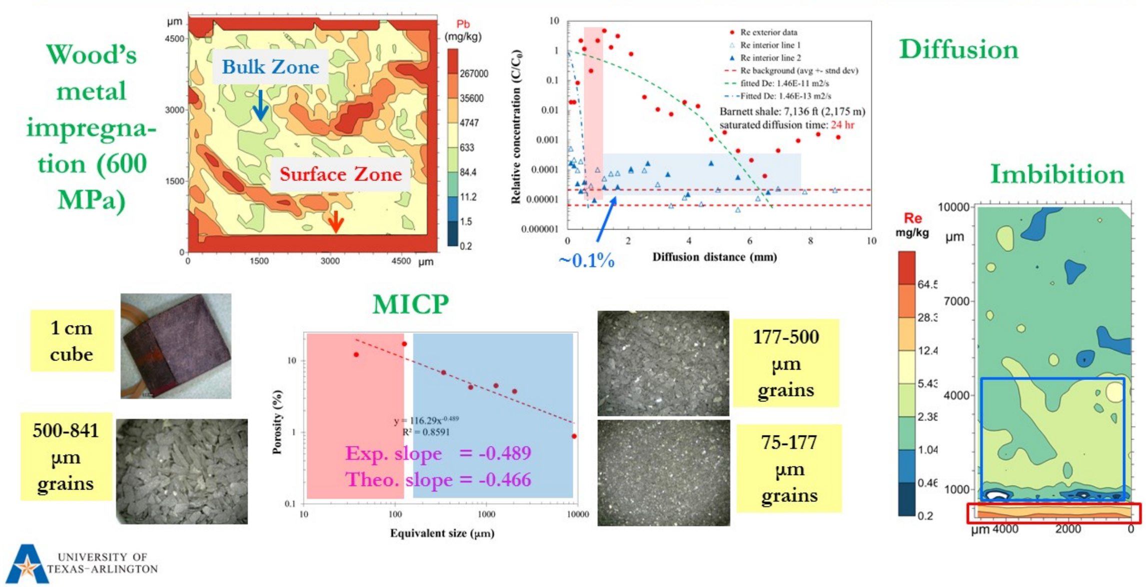

RESULTS (SCATTERING) & CONCLUSIONS

Small Angle Neutron Scattering (SANS)

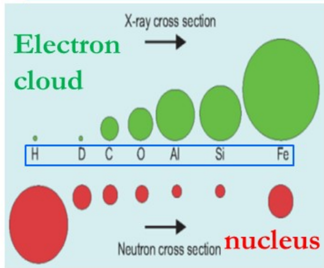

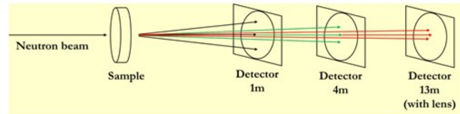

- Detect both connected and closed pores
- Obtain full-scale nm-μm pore diameters
- Quantify hydrophilic vs. hydrophobic pore space
- Investigate reservoir P-T condition

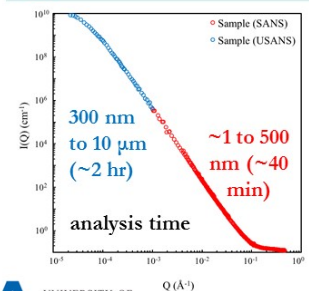

UNIVERSITY OF TEXAS-ARLINGTON

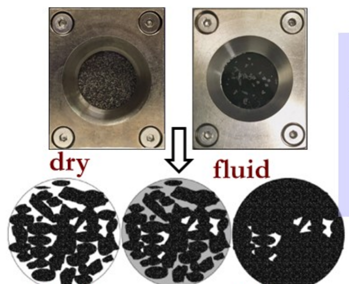

Contrast matching
d-H_2O
d-2DT
d-IPA

- Yang et al., Fuel, 2017
- Sun et al., IJCG, 2017
- Zhao et al., SR, 2017
- Zhang et al., MPG, 2019

YMP Welded Tuff: (U)SANS and Other Results

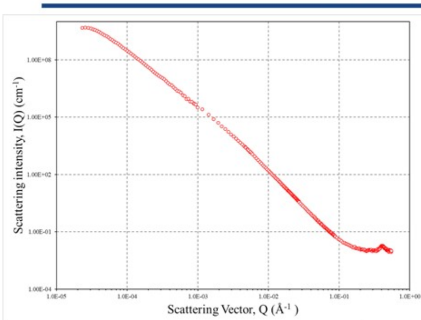

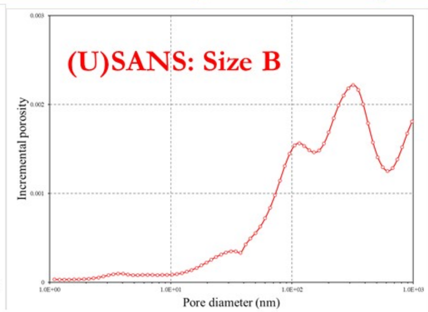

Pore diameter	Porosity (%)
1-2 nm	0.02
2-50 nm	0.61
50-100 nm	0.71
100 nm-1 μm	4.18
Total	5.52

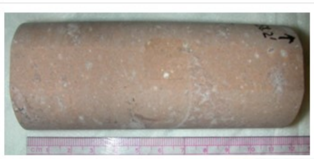

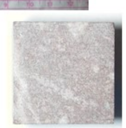

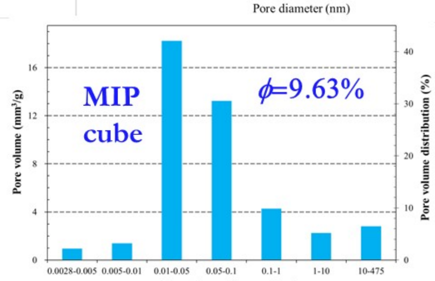

FIP (cubes): 9.11±0.05%

UNIVERSITY OF TEXAS-ARLINGTON

Wolfcamp Shale: (U)SANS and Other Results

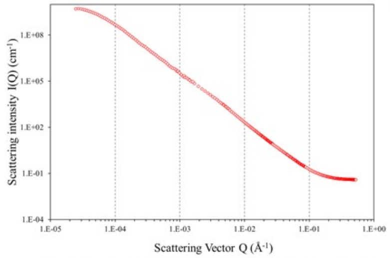

SANS: grains (177-500 μm)

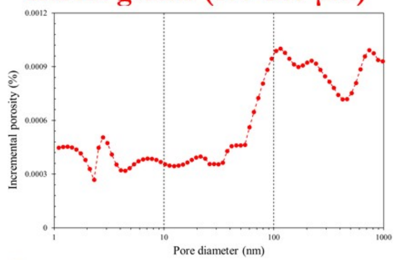

Pore diameter (μm)	MIP (2.8 nm - 50 μm)		SANS (1 nm - 20 μm)		Pore body : cavity ratio
	Porosity (%)	Porosity distri-bution (%)	Porosity (%)	Porosity distri-bution (%)	
0.0001-0.0028			0.459	10.5	
0.0028-0.005	0.783	16.4	0.239	5.49	0.33
0.005-0.01	1.05	22.1	0.28	6.45	0.29
0.01-0.05	1.00	20.9	0.66	15.1	0.72
0.05-0.1	0.365	7.64	0.553	12.7	1.7
0.1-1	1.57	33.0	2.17	49.8	1.5
Total	4.77		4.35		

FIP (cylinder & cubes) porosity: 2.93±0.15%

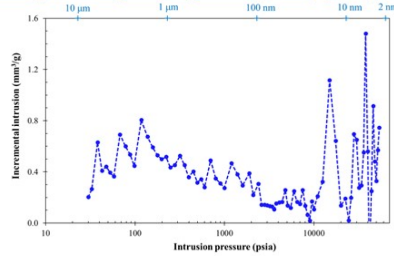

MIP: grains (177-500 μm)

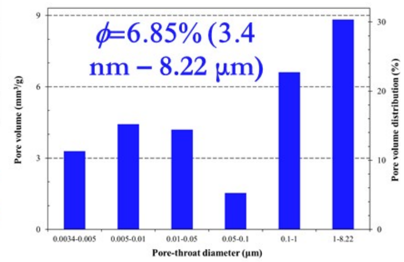

UNIVERSITY OF TEXAS–ARLINGTON

Japan Wakkanai Mudstone: USANS and Other Results

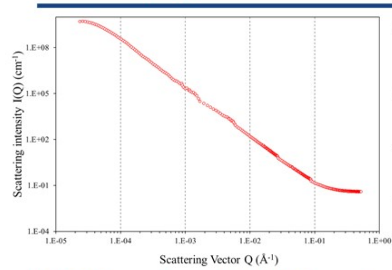

SANS: grains (177-500 μm)

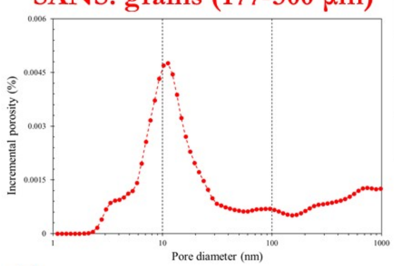

Pore diameter (μm)	MIP (2.8 nm - 50 μm)		SANS (1 nm - 20 μm)		Pore body : cavity ratio
	Porosity (%)	Porosity distri-bution (%)	Porosity (%)	Porosity distri-bution (%)	
0.0001-0.0028			0.063	0.710	
0.0028-0.005	0.0662	0.235	0.612	6.90	29.3
0.005-0.01	5.29	18.8	2.24	25.3	1.3
0.01-0.05	11.6	41.3	3.31	37.3	0.9
0.05-0.1	4.47	15.9	0.497	5.60	0.4
0.1-1	6.69	23.8	2.15	24.2	1.0
Total	28.1		8.87		

FIP (cylinders & cubes) porosity: 34.6±0.66%

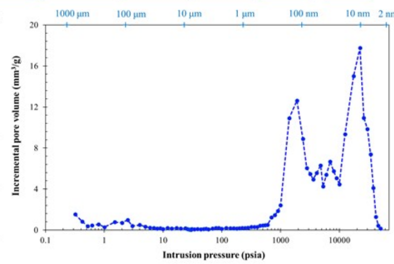

MIP: cube (1 cm)

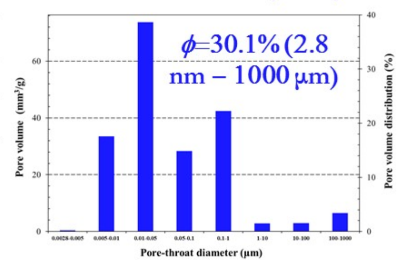

UNIVERSITY OF TEXAS–ARLINGTON

X-ray Scattering Application

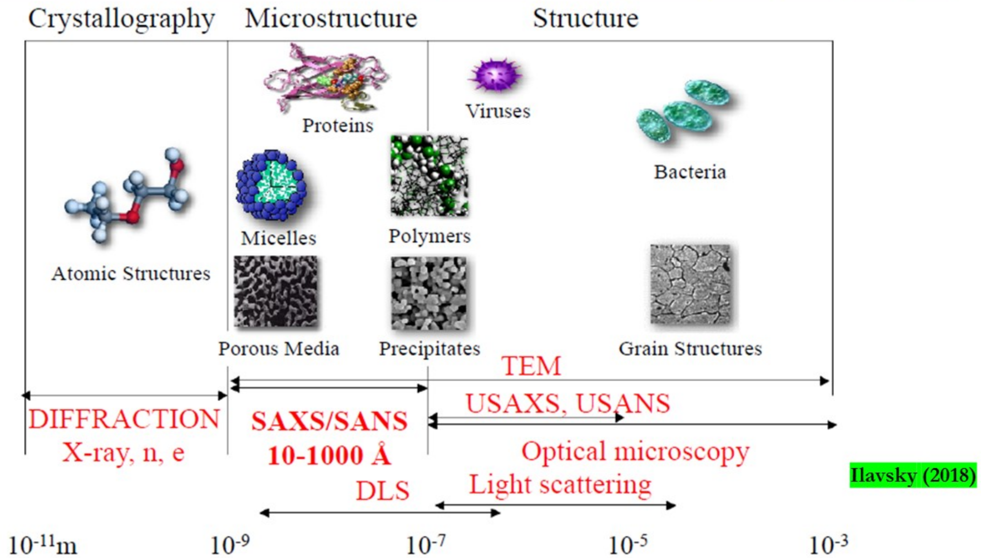

UNIVERSITY OF TEXAS–ARLINGTON

Advanced Photon Sources (APS)

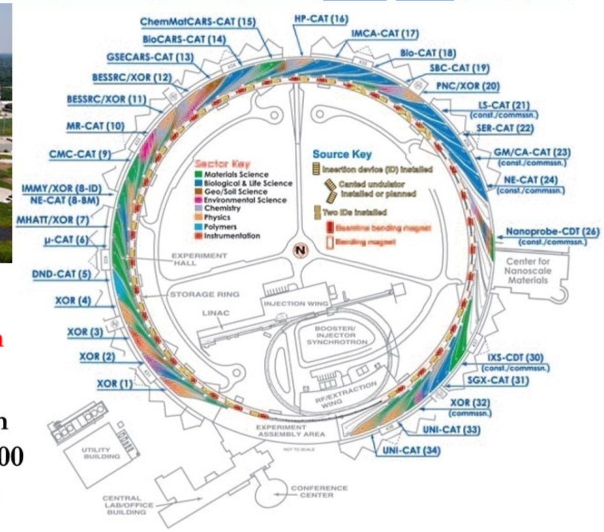

- 80-acre site; ~450 employees
- The brightest x-ray beams in the Western Hemisphere
- The largest of the 5 DOE light sources in terms of users per year for more than 5,000 (and growing) scientists from around the United States and the world

UNIVERSITY OF TEXAS–ARLINGTON

http://www.aps.anl.gov/

9-ID: USAXS/SAXS/WAXS

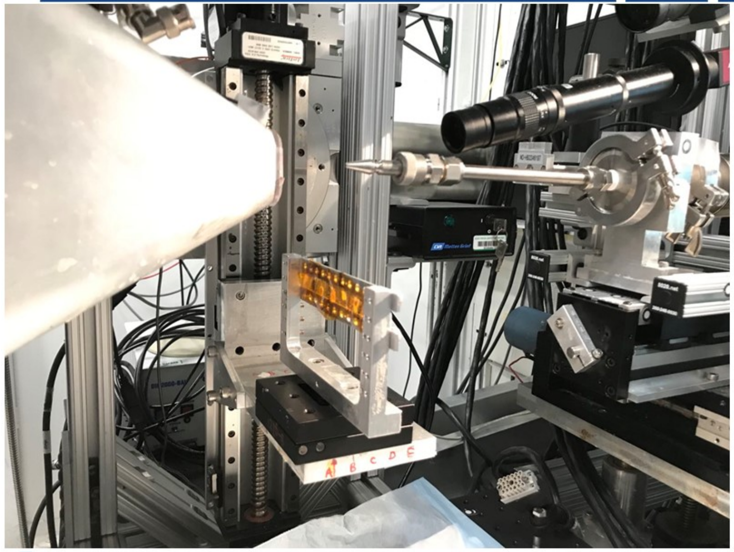

- Energy range: 10-24 keV
- Beam size:
- Analytical time: 4-5 min one position

"New user and joint SANS/SAXS proposals on pore connectivity studies of shale gas and oil reservoirs" (2 days of 9-ID, 8/2020)

Jan Ilavsky

UNIVERSITY OF TEXAS–ARLINGTON

https://youtu.be/-a9nD4W2ShQ

26

Sample Preparation: Solid Form and Thickness

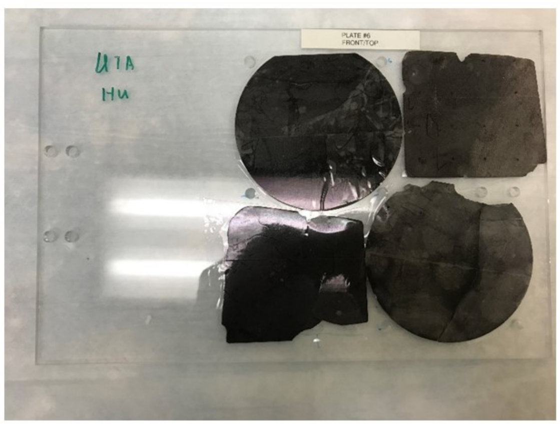

Whole core wafers: height= 0.5~0.8 mm

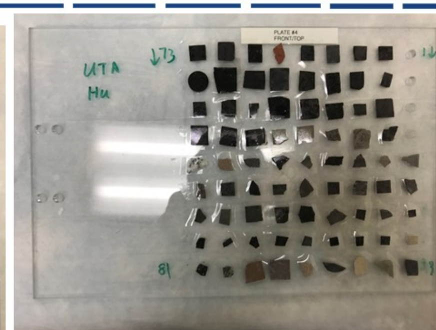

~1 cm wafer: height @ 0.5~0.8 mm

(Micro) Cuvettes: granular sample thickness @ 0.5, 1, and 4 mm

UNIVERSITY OF TEXAS–ARLINGTON

High-Energy SAXS/WAXS at 1-1D

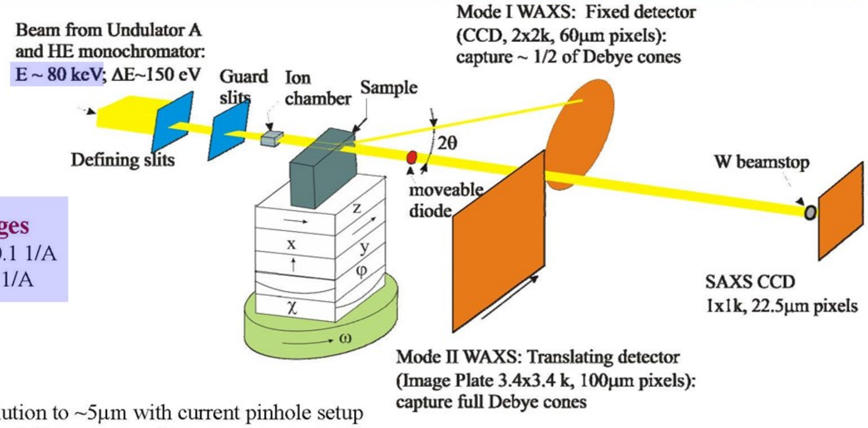

Typical q-ranges
- SAXS: 0.002-0.1 1/A
- WAXS = 0.2-5 1/A

Features
- *Direct* depth resolution to ~5μm with current pinhole setup
- Strong penetration ability: comparable to neutrons
- Perform WAXS,SAXS (and imaging) with little change in setup
- $t_{exposure}$~ 1-100 sec (both WAXS and SAXS)
- Plan to incorporate refractive-lens focusing optics (late 2004):
  - anticipate q(min) to ~ 0.0005 1/A
  - 1-D spatial resolution to ~1μm

✓ Jon Almer

✓ Jun-Sang Park

UNIVE TEXAS-.

Sample Preparation: Form and Thickness

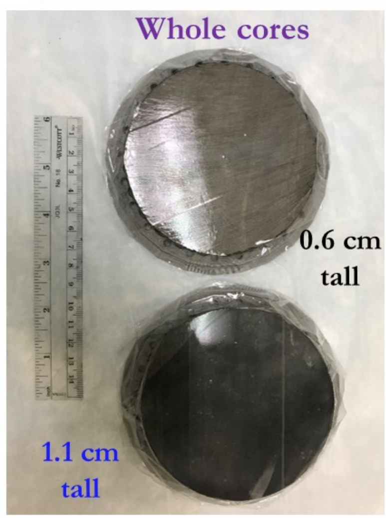

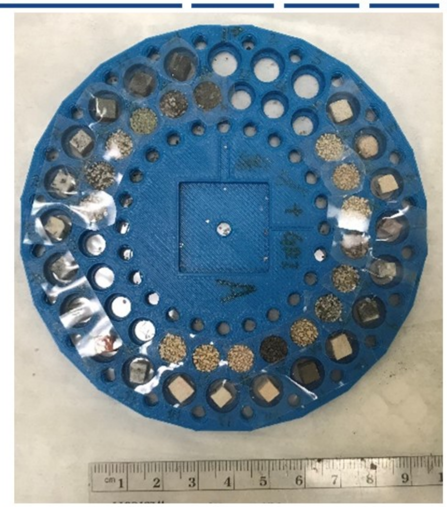

- granular
- non-granular

"New user and joint SANS/SAXS proposals on pore connectivity studies of shale gas and oil reservoirs" (2 days of 9-ID WAXS/SAXS/USAXS, 8/2020)

UNIVERSITY OF TEXAS-ARLINGTON

Summary

- A variety of generic barrier materials are studied
- Dual connectivity zones are observed for mudrock
- Pore structure, especially pore connectivity, influences fluid flow and chemical transport in low-permeability media
- Limited pore connectivity will be conductive to enhanced diffusion and retention of radionuclides in barrier materials

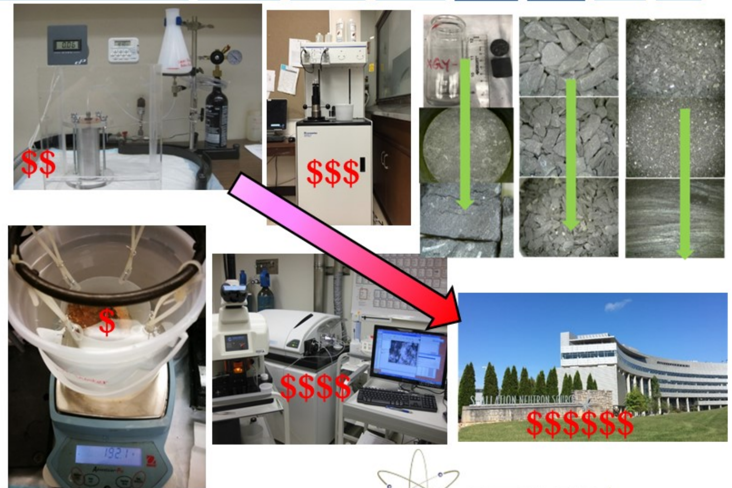

UNIVERSITY OF TEXAS-ARLINGTON

JAEA Japan Atomic Energy Agency

NEUP Nuclear Energy University Program
U.S. Department of Energy

Acknowledgments

RPSEA Research Partnership to Secure Energy for America
ConocoPhillips
JAEA Japan Atomic Energy Agency
SINOPEC
NEUP Nuclear Energy University Program
U.S. Department of Energy

USGS science for a changing world
Bureau of Economic Geology
New Mexico Bureau of Geology and Mineral Resources
North Dakota Geological Survey
O.D.N.R. Geological Survey
Diamondback Energy
Pennsylvania Geological Survey
Vitruvian Exploration
element petroleum III, llc
Pioneer Natural Resources
Exxon XTO Energy

Leibniz Universität Hannover
EMPA Materials Science & Technology
Iowa State University
Oak Ridge National Laboratory
NIST

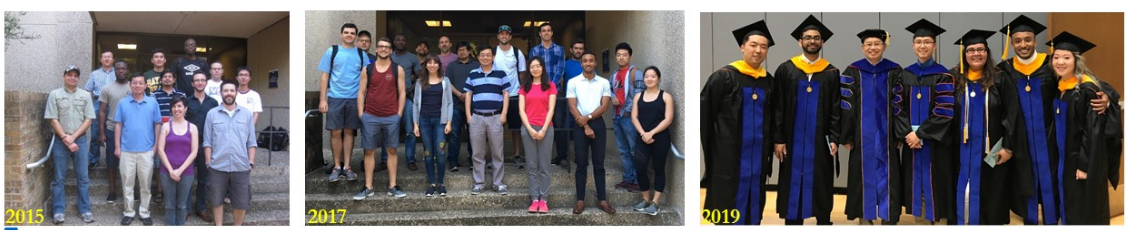

UNIVERSITY OF TEXAS-ARLINGTON

ABSTRACT

Pore connectivity, a topological characteristic of pore structure, is oftentimes more important than the geometrical aspects in controlling fluid flow and mass transport in porous natural rocks as well as their associated utilities in energy and environmental stewardship. A different extent of pore connectivity can be reflected in the proportion of isolated pore space not connected to the surface of natural rocks. This work presents the multi-approach and multi-scale laboratory studies to investigating the proportion of isolated pore space of, and its resultant anomalous fluid flow and radionuclide movement in, generic geological barrier materials (clay sediment, crystalline rock, salt rock, shale, tuff). The samples include clay sediments of Wakkanai formation at Horonobe underground research center in Hokkaido of Japan, Opalinus clay of Mt. Terri Underground Research Laboratory as well as granodiorite from the Grimsel Test Site in Switzerland, salt rock from Waste Isolation Pilot Plant in New Mexico, various shales (Barnett, Eagle Ford and Wolfcamp from Texas), and welded tuff in Yucca Mountain in Nevada. Working with sample sizes from <75 μm to several centimeters, the experimental approaches include the independent quantification of both (1) surface-accessible pore space with various probing fluids (e.g., helium in expansion, water in vacuum saturation and nuclear magnetic resonance, mercury in intrusion porosimetry, nitrogen in gas physisorption, and Wood's metal in high-pressure impregnation and micron-scale tracer mapping using laser ablation-ICP-MS); and (2) total (both connected and isolated) porosity by small angle X-ray scattering. In summary, our evolving complementary approaches provide a rich toolbox for tackling the pore structure characteristics in geological barrier materials, and associated fluid flow & radionuclide transport, implicated in their long-term performance in natural and engineered systems of a nuclear waste repository.

Acknowledgements: This project was completed with funding provided by the Nuclear Energy University Program of Office of Nuclear Energy at the U.S. Department of Energy (award number DE-NE0008797) and Japan Atomic Energy Agency.